Acceleration mechanism responsible for the formation of the new radiation belt during the 2003 Halloween solar storm

Y. Y. Shprits,[1] R. M. Thorne,[1] R. B. Horne,[2] S. A. Glauert,[2] M. Cartwright,[3] C. T. Russell,[3] D. N. Baker,[4] and S. G. Kanekal[4]

Received 2 August 2005; revised 20 December 2005; accepted 13 January 2006; published 11 March 2006.

[1] Observations of the relativistic electron flux increases during the first days of November, 2003 are compared to model simulations of two leading mechanisms for electron acceleration. It is demonstrated that radial diffusion driven by ULF waves cannot explain the formation of the new radiation belt in the slot region and instead predicts a decay of fluxes during the recovery phase of the October 31st storm. Compression of the plasmasphere during the main phases of the storm created preferential conditions for local acceleration during interactions with VLF chorus. Local acceleration of electrons at $L = 3$ is modelled with a 2-D pitch-angle, energy diffusion code. We show that the energy diffusion driven by whistler mode waves can explain the gradual build up of fluxes to energies exceeding 3 MeV in a new radiation belt which is formed in the slot region normally devoid of high energy electrons. **Citation:** Shprits, Y. Y., R. M. Thorne, R. B. Horne, S. A. Glauert, M. Cartwright, C. T. Russell, D. N. Baker, and S. G. Kanekal (2006), Acceleration mechanism responsible for the formation of the new radiation belt during the 2003 Halloween solar storm, *Geophys. Res. Lett.*, *33*, L05104, doi:10.1029/2005GL024256.

1. Introduction

[2] The Halloween storms of October–November, 2003 were one of the most dramatic examples of intense Sun-Earth connection over the last decade [*Lopez et al.*, 2004]. During this event, which was initiated by two large coronal mass ejections, the plasmapause was compressed inside $L = 2$ (for several days) and an entirely new relativistic electron population was accelerated or injected into the "slot" region between $2.5 < L < 3.5$ [*Baker et al.*, 2004], which is normally devoid of intense particle flux [e.g., *Lyons and Thorne*, 1973]. The unprecedented geomagnetic storms of October–November 2003 provided unique conditions when acceleration due to these two leading acceleration mechanisms was separated both in time and space.

[3] The outer radiation belt exhibits a significant variability due to competing source and loss processes which act on a similar time scales. Leading mechanisms for acceleration to relativistic energies include radial diffusion driven by ULF waves [e.g., *Elkington et al.*, 2003], local stochastic acceleration driven by VLF waves [*Horne and Thorne*, 1998; *Summers et al.*, 1998; *Horne et al.*, 2005a], and rapid shock induced acceleration [*Li et al.*, 1993], which was ineffective during these storm events. The loss of relativistic electrons is due to pitch-angle scattering by EMIC waves [*Thorne and Kennel*, 1971; *Lyons and Thorne*, 1972; *Meredith et al.*, 2003], chorus waves outside the plasmapause [*O'Brien et al.*, 2004; *Thorne et al.*, 2005b] and plasmaspheric hiss [*Abel and Thorne*, 1998]. Losses to the magnetopause during the main phase of a storm [*Selesnick and Blake*, 2000] may also contribute to net loss by creating inward gradients in phase space density which transport electrons outward. Outward radial diffusion conserving the first two adiabatic invariants will decelerate particles and essentially works as an effective loss mechanism over a wide range of L values in the outer magnetosphere.

[4] Dramatic intensifications of relativistic electron flux in the slot region ($2.5 \leq L \leq 3.5$), typically deficient of high energy electrons, was reported from observations on the Solar, Anomalous, and Magnetospheric Particle Explorer (SAMPEX) satellite [*Baker et al.*, 2004], but a comprehensive physical explanation for such an unusual behavior of the radiation belts was not given. Here we present model simulations of the two potential acceleration processes and identify which is dominant during the recovery phase of these intense storms.

2. Observations of the Formation of a New Radiation Belt in the Slot Region

[5] Figure 1A shows electron fluxes at energies 2–6 MeV observed on SAMPEX, plotted in terms of time and L-shell. Clearly evident are the strong depletions in relativistic electron flux during October 29 and October 31. The unusual new radiation belt reaches maximum intensity during the first days of November, with fluxes gradually building up until the 3rd of November, followed by a slow decay and a reformation of the outer radiation belt after November 10 at its typical location (around 4 R_E). Since *Dst* almost recovers by November 1, (Figure 1D, *Dst* is −72 nT at 0:30 on November 1 and is −32 nT at 0:30 on November 3rd) such small variations in the magnetic field at $L = 2–3$, where the background magnetic field is very strong, cannot have a significant effect on the evolution of fluxes. Figure 1C depicts the evolution of the *Kp* index, which is very high during October 29 and October 31, but is moderate-to-low when the new belt reaches maximum intensity on November 1–2. Figure 1B shows compressional ULF wave power in the Pc5 frequency range observed by the Polar satellite. To clean the data we

[1]Department of Atmospheric and Oceanic Sciences, University of California, Los Angeles, California, USA.
[2]British Antarctic Survey, Cambridge, UK.
[3]Department of Earth and Space Sciences, University of California, Los Angeles, California, USA.
[4]Laboratory for Atmospheric and Space Physics, Boulder, Colorado, USA.

Copyright 2006 by the American Geophysical Union.
0094-8276/06/2005GL024256$05.00

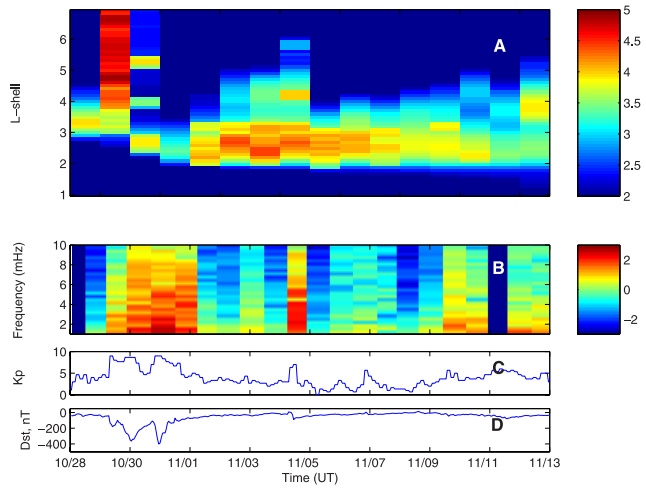

Figure 1. Observations of the global magnetospheric response to the October–November 2003 solar storms. (A) Daily averaged electron fluxes at energies 2.0–6.0 MeV in ($\log_{10}$ (cm^2 sr sec)$^{-1}$) measured on SAMPEX spacecraft as a function of time and L-shell, from October 28 to November 14, 2003. The gradual build up of fluxes between 2 and 3 Earth radii primarily occurs from November 1–3, followed by a slow decay and reformation of the outer radiation belt at its typical location around 4–5 Earth radii. (B) Log of the compressional ULF Pc 5 power in $\log_{10}$(nT^2/Hz) measured on the Polar spacecraft averaged over a range of L-shells from 2.5–6 Re. ULF wave power is obtained only when Polar is within 20 degrees in latitude from equator. (C) Evolution of the *Kp* index. (D) Evolution of the *Dst* index.

removed data spikes, data gaps, and performed liner interpolation. The T96 [*Tsyganenko and Stern*, 1996], model field was subtracted off and the resulting data was detrended. Potential inaccuracies associated with subtracting a quiet time field model would only increase the depicted wave power during the most active periods. We then used a 512-point FFT with a one hour sliding window to analyze the wave power. In the analysis we considered only data points when Polar was between 2.5 and 6 R_E and within twenty degrees from equator. The data points obtained were then averaged over half an orbit. As a result the wave power is an average over a range of L-shells, and is representative of the overall ULF activity during these days. While ULF waves activity is very strong during the onset of the storms on October 29–31, the wave power is very low during the period when the slot region electron flux enhancement is the most pronounced (November 1 and 2). Similar increases in Pc5 wave power during the main phases of the storms and dropout in the recovery phase were observed on the ground [*Horne et al.*, 2005b], which shows that none of the excited ULF modes is likely to have a significant power on November 1, and 2. Compressional ULF power also closely follows the evolution of the *Kp* index, very high values on October 29 and October 31, followed by a pronounced drop during the first few days of November.

3. Radial Diffusion Modeling

[6] The effect of the decrease in radial diffusion coefficients associated with a decrease in ULF wave power, is illustrated schematically in Figure 2. Radial diffusion modeling yields a monotonic increase in phase space density with increasing L, if the outer boundary is relatively constant. In the outer region (diffusion dominated region), the time scales associated with the radial diffusion are expected to be shorter than loss time scales, producing flat phase space density profile. At lower L losses become dominant and produce a sharp drop in phase space density (loss dominated region). A decrease in the rate of radial diffusion will move the diffusion dominated region outward and will result in a decrease in fluxes in the slot region [*Thorne*, 1982; *Shprits and Thorne*, 2004]. To illustrate that radial diffusion is not capable of explaining the build up of fluxes during the November 1–3 period in the slot region, we carry out a radial diffusion simulation with lifetimes parameterized as $\tau = 3/Kp$ [*Shprits et al.*, 2005], and solve the radial diffusion equation (1) [*Schulz and Lanzerotti*, 1974], with *Kp* dependent diffusion coefficients D_{LL}, derived by *Brautigam and Albert* [2000].

$$\frac{\partial f}{\partial t} = L^2 \frac{\partial}{\partial L}\left[D_{LL}L^{-2}\frac{\partial f}{\partial L}\right] - \frac{f}{\tau} \qquad (1)$$

[7] For this simplified simulation, following [*Shprits and Thorne*, 2004] we take constant outer boundary condition at $L = 7$ and initial conditions derived from the SAMPEX measurements on the November 1. The assumption of the constant outer boundary fluxes is justified by the LANL satellite measurements, which do not show significant flux variations at geosynchronous orbit during the modeled period. To obtain the boundary conditions we use a dipole field, and average electron fluxes at the outer boundary, which despite inaccuracies at high L values produces substantial flux in the slot region on November 1 (Figure 3) and provides a fair test of the radial diffusion mechanism. Figure 3 shows the result of the radial diffusion simulation, over a 2 day period (November 1–3). Instead of the observed gradual build up of fluxes in the new radiation belt above $L = 2$, radial diffusion predicts a flux decay due to the pronounced drop in ULF wave activity. Furthermore, acceleration caused by radial diffusion should have been

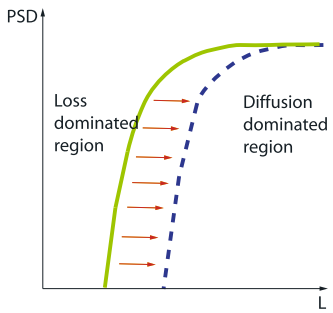

Figure 2. Illustration of the effect of the decrease in ULF activity and consequent decrease in diffusion coefficients. The green solid line corresponds to PSD during high geomagnetic activity, dashed blue line corresponds to a PSD during quiet times. The region of high gradients in PSD moves to higher L values when ULF power decreases, which results in a drop in fluxes at lower L-values when the ULF activity drops.

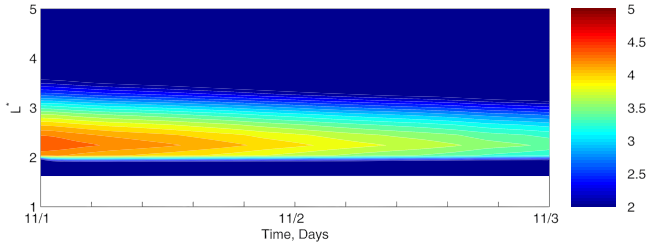

Figure 3. Results of a two day radial diffusion simulation starting on November 1. Radial diffusion predicts a decay of fluxes contrary to observations which show a gradual build up of relativistic electron flux in the slot region.

most effective during the onsets of the storms on October 29, 31 and November 4, 20 whereas observations indicate flux depletions, possibly due to enhanced precipitation losses or enhanced outward radial diffusion. Clearly radial diffusion cannot explain the formation of a new radiation belt in the slot region during the storm recovery (November 1–3).

4. Local Acceleration

[8] The gradual build up of relativistic electron flux in the storm recovery phase can be explained by wave-particle interaction with enhanced Very Low Frequency (VLF) chorus emission [*Meredith et al.*, 2003]. Such waves, which are excited throughout the low-density region exterior to the plasmasphere are capable of causing local acceleration [*Horne et al.*, 2005a]. Because of the extreme compression of the plasmapause [*Baker et al.*, 2004] during these superstorms, the local acceleration process should have been operative down to $L = 2$, where it becomes very efficient [*Horne et al.*, 2005a].

[9] To examine the viability of local acceleration we carried out a two-dimensional simulation of pitch-angle and energy diffusion, solving equation (2) over the storm recovery phase (November 1–3) at $L = 3$. Ignoring radial diffusion, violation of the first two adiabatic invariants μ and J, leading to diffusion in pitch-angle and momentum p, can be modelled using a modified Fokker-Planck equation:

$$\frac{\partial f}{\partial t} = \frac{1}{p^2}\frac{\partial}{\partial p}p^2 D_{pp}\frac{\partial f}{\partial p} + \frac{1}{p^2}\frac{\partial}{\partial p}p^2 D_{py}\frac{\partial f}{\partial y} + \frac{1}{T(y)y}\frac{\partial}{\partial y}T(y)yD_{py}\frac{\partial f}{\partial p} + \frac{1}{T(y)y}\frac{\partial}{\partial y}T(y)yD_{yy}\frac{\partial f}{\partial y} \quad (2)$$

where $y = \sin(\alpha)$, and $T(y) = 1.3802 - 0.3198*(y + y^{1/2})$. The magnitude of the mixed diffusion terms D_{py} can become comparable to the pure pitch-angle and energy terms [*Horne et al.*, 2005a], but will not exceed the largest of the terms. Recent results by *Albert and Young* [2005] show that the inclusion of mixed terms may contribute up to a factor of five at lower pitch angles but will not substantially change flux near $\alpha = \pi/2$. Consequently, in this study we ignore the computationally expensive and complicated effects of the mixed diffusion.

[10] To compute energy and pitch-angle diffusion coefficients we use the PADIE (Pitch Angle and Energy Diffusion of Ions and Electrons) diffusion code [*Glauert and Horne*, 2005]. The results of the code have been verified against a similar code [*Albert*, 2003, 2005]. Following *Thorne et al.* [2005a] we adopt realistic parameters for the stormtime properties of lower band equatorial chorus ($\omega_m = 0.35\Omega_e$, $\delta\omega = 0.15\Omega_e$, $B_w = 50$ pT), assuming a Gaussian distribution with peak value of B_w at ω_m and cut offs at $\omega_m \pm 2\delta\omega$, based on the statistical study of [*Meredith et al.*, 2003]. $N = 100$ cm^{-3}, is used to simulate equatorial conditions outside the plasmapause at $L = 3$ [*Sheeley et al.*, 2001]. Evidence of enhanced chorus activity during the first two days of November comes from a variety of sources: ground measurements at Palmer station [*Spasojevíc and Inan*, 2005; *Horne et al.*, 2005b] and observations on Cluster spacecraft ($L \geq 4.5$) [*Horne et al.*, 2005b]. The boundary conditions on PSD as a function of pitch angle is $f(\alpha = 0°) = 0$ and $\partial f/\partial\alpha(\alpha = 90°) = 0$. The lifetimes are assumed to be infinite outside of the loss cone and are set to a quarter bounce time period inside of the loss cone. The lower boundary in energy is fixed at 150 keV (to simulate convective source) and the upper boundary is set to 0 at 15 MeV. We first initialize the code by running it for 2 days to produce initial conditions similar to those observed on November 1st, starting with a typical slot region energy distribution function. Figure 4 shows the evolution of the modeled nearly equatorial ($\alpha = 80°$) fluxes as a function of energy. The gradual acceleration of electrons during the 2 days of the simulation at $L = 3$ is reasonably consistent with SAMPEX observations for relativistic electron fluxes above 2 MeV.

5. Discussion

[11] During the period October 29–31 enhanced ULF wave power may drive inward radial diffusion inside the local peak in PSD and outward radial diffusion outside of the peak in PSD. The gradients in phase space density may be created by the local acceleration source, losses in the slot region and losses to magnetopause. Since both local acceleration and radial diffusion may have contributed to the variability of the outer belt electron fluxes during the storms main phase (October 29, 31) in this study we concentrate on the numerical modelling of acceleration of electrons in the recovery phase of these storms (November 1, 2), when the slot region fluxes were most enhanced.

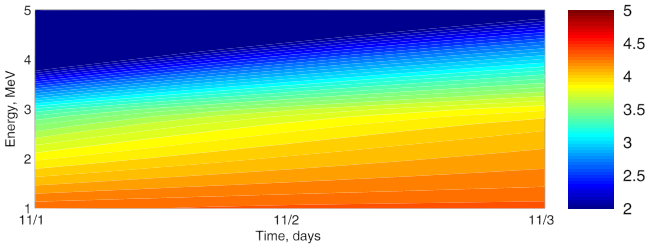

Figure 4. Results of a two day simulation (starting on November 1) of the build up of relativistic electron flux due to local acceleration at $L = 3$. The horizontal axis is time in the simulation, the vertical axis is the electron energy. Electron fluxes, color coded in $\log_{10}$ (cm sr sec MeV)$^{-1}$, build up continuously throughout the simulation and reach levels similar to those observed on SAMPEX at 2 MeV.

[12] During the recovery phase of the Halloween storms the plasmasphere was drastically compressed for several days down to 2 Earth radii. This created unprecedented conditions (strong magnetic field and low plasma densities) for the local acceleration, while ULF activity was low. Model results described above show that the formation of the new belt during this time could be produced by local acceleration alone. However, radial diffusion might have significantly contributed to smoothing the peaks in phase space density and accelerating elections inside the local peak while producing significant losses in the outer region. The observed decreases in the outer radiation belt fluxes during the onsets of the storms on October 29, 31, November 4, 20 could be explained by enhanced losses and outward radial diffusion driven by inward gradients in phase space density. Radial diffusion may also contribute to acceleration of electrons inside of the peak in phase space density, during the main phases of the storms and may be also responsible for the radial diffusion of the electrons from the slot region into the inner zone following the storm. Future research should address the development of three dimensional codes incorporating radial diffusion, local acceleration and stormtime losses.

[13] **Acknowledgment.** This study was supported by the NSF grant ATM -0402615 and NASA grants NNG04GN44G and NAG5-11324.

References

Abel, B., and R. M. Thorne (1998), Electron scattering loss in Earth's inner magnetosphere: 1. Dominant physical processes, *J. Geophys. Res.*, *103*, 2385–2396.

Albert, J. M. (2003), Evaluation of quasi-linear diffusion coefficients for EMIC waves in a multispecies plasma, *J. Geophys. Res.*, *108*(A6), 1249, doi:10.1029/2002JA009792.

Albert, J. M. (2005), Evaluation of quasi-linear diffusion coefficients for whistler mode waves in a plasma with arbitrary density ratio, *J. Geophys. Res.*, *110*, A03218, doi:10.1029/2004JA010844.

Albert, J. M., and S. L. Young (2005), Multidimensional quasi-linear diffusion of radiation belt electrons, *Geophys. Res. Lett.*, *32*, L14110, doi:10.1029/2005GL023191.

Baker, D. N., S. G. Kanekal, X. Li, S. P. Monk, J. Goldstein, and J. L. Burch (2004), An extreme distortion of the Van Allen belt arising from the Halloween solar storm in 2003, *Nature*, *432*, 878–880.

Brautigam, D. H., and J. M. Albert (2000), Radial diffusion analysis of outer radiation belt electrons during the October 9, 1990 magnetic storm, *J. Geophys. Res.*, *105*(A1), 291–310.

Elkington, S. R., M. K. Hudson, and A. A. Chan (2003), Resonant acceleration and diffusion of outer zone electrons in a n asymmetric geomagnetic field, *J. Geophys. Res.*, *108*(A3), 1116, doi:10.1029/2001JA009202.

Glauert, S. A., and R. B. Horne (2005), Calculation of pitch angle and energy diffusion coefficients with the PADIE code, *J. Geophys. Res.*, *110*, A04206, doi:10.1029/2004JA010851.

Horne, R. B., and R. M. Thorne (1998), Potential waves for relativistic electron scattering and stochastic acceleration during magnetic storms, *Geophys. Res. Lett.*, *25*(15), 3011–3014.

Horne, R. B., R. M. Thorne, S. A. Glauert, J. M. Albert, N. P. Meredith, and R. R. Anderson (2005a), Timescales for radiation belt electron acceleration by whistler mode chorus, *J. Geophys. Res.*, *110*, A03225, doi:10.1029/2004JA010811.

Horne, R. B., et al. (2005b), Wave acceleration of electrons in the Van Allen radiation belts, *437*, 227–230, doi:10.1038/nature03939.

Li, X., I. Roth, M. Temerin, J. R. Wygant, M. K. Hudson, and J. B. Blake (1993), Simulation of the prompt energization and transport of radiation belt particles during the March 24, 1991 SSC, *Geophys. Res. Lett.*, *20*(22), 2423–2426, doi:10.1029/1993GL02701.

Lopez, R. E., D. N. Baker, and J. H. Allen (2004), Sun unleashes Halloween storm, *Eos Trans. AGU*, *85*, 105–108.

Lyons, R. L., and R. M. Thorne (1972), Parasitic pitch angle diffusion of radiation belt particles by ion cyclotron waves, *J. Geophys. Res.*, *77*, 5608–5615.

Lyons, R. L., and R. M. Thorne (1973), Equilibrium structure of radiation belt electrons, *J. Geophys. Res.*, *78*, 2142–2149.

Meredith, N. P., R. M. Thorne, R. B. Horne, D. Summers, B. J. Fraser, and R. R. Anderson (2003), Statistical analysis of relativistic electron energies for cyclotron resonance with EMIC waves observed on CRRES, *J. Geophys. Res.*, *108*(A6), 1250, doi:10.1029/2002JA009700.

O'Brien, T. P., M. D. Looper, and J. B. Blake (2004), Quantification of relativistic electron microbursts losses during the GEM storms, *Geophys. Res. Lett.*, *31*, L04802, doi:10.1029/2003GL018621.

Schulz, M., and L. J. Lanzerotti (1974), *Particle Diffusion in the Radiation Belts*, vol. 7, *Physics and Chemistry in Space*, Springer, New York.

Selesnick, R. S., and J. B. Blake (2000), On the source location of radiation belt relativistic electrons, *J. Geophys. Res.*, *105*(A2), 2607–2624.

Sheeley, B. W., M. B. Moldwin, H. K. Rassoul, and R. R. Anderson (2001), An empirical plasmasphere and trough density model: CRRES observations, *J. Geophys. Res.*, *106*(A11), 25,631–25,642.

Shprits, Y. Y., and R. M. Thorne (2004), Time dependent radial diffusion modeling of relativistic electrons with realistic loss rate, *Geophys. Res. Lett.*, *31*, L08805, doi:10.1029/2004GL019591.

Shprits, Y. Y., R. M. Thorne, G. D. Reeves, and R. Friedel (2005), Radial diffusion modeling with empirical lifetimes: Comparison with CRRES observations, *Ann. Geophys.*, *23*, 1467–1471.

Spasojevíc, M., and U. S. Inan (2005), Ground based VLF observations near L = 2.5 during the Halloween 2003 storm, *Geophys. Res. Lett.*, *32*, L21103, doi:10.1029/2005GL024377.

Summers, D., R. M. Thorne, and F. Xiao (1998), Relativistic theory of wave-particle resonant diffusion with application to electron acceleration in the magnetosphere, *J. Geophys. Res.*, *103*(A9), 20,487–20,500.

Thorne, R. M. (1982), Injection and loss mechanisms for energetic ions in the inner Jovian magnetosphere, *J. Geophys. Res.*, *82*, 8105–8110.

Thorne, R. M., and C. F. Kennel (1971), Relativistic electron precipitation during magnetic storm main phase, *J. Geophys. Res.*, *76*, 4446–4453.

Thorne, R. M., Horne, S. Glauert, N. Meredith, Y. Y. Shprits, D. Summers, and R. Anderson (2005a), The influence of wave-particle interactions on relativistic electron dynamics during storms, in *Inner Magnetosphere Interaction: New Perspectives from Imaging*, *Geophys. Monogr. Ser.*, vol. 159, edited by J. Burch, M. Schulz, and H. Spence, AGU, Washington, D. C.

Thorne, R. M., T. P. O'Brien, Y. Y. Shprits, D. Summers, and R. B. Horne (2005b), Timescale for MeV electron microburst loss during storms, *J. Geophys. Res.*, *110*, A09202, doi:10.1029/2004JA010882.

Tsyganenko, N. A., and D. P. Stern (1996), Modeling the global magnetic field of the large-scale Birkeland current systems, *J. Geophys. Res.*, *101*(A12), 27,187–27,198.

D. N. Baker and S. G. Kanekal, Laboratory for Atmospheric and Space Physics, Boulder, CO 80309-0590, USA.

M. Cartwright and C. T. Russell, Department of Earth and Space Sciences, University of California, Los Angeles, CA 90095, USA.

S. A. Glauert and R. B. Horne, British Antarctic Survey, Cambridge, CB3 0ET, UK.

Y. Y. Shprits and R. M. Thorne, Department of Atmospheric and Oceanic Sciences, University of California, Los Angeles, CA 90095, USA. (yshprits@atmos.ucla.edu)